PROCEEDINGS OF SCIENCE

CPV and CKM at Belle II: status and prospects

Michele Mantovano[a,b,*]

[a] *Dipartimento di Fisica, Università di Trieste, I-34127 Trieste, Italy*
[b] *INFN Sezione di Trieste, I-34127 Trieste, Italy*

E-mail: michele.mantovano@ts.infn.it

We present recent measurements relevant to the CKM unitarity triangle and CP violation, based on data collected by the Belle II experiment at the $\Upsilon(4S)$ resonance from 2019 to 2022. These measurements play a crucial role in testing the consistency of the Standard Model and probing possible signs of new physics. Specifically, we report the latest results on two-body B-meson decays contributing to the determination of the CKM angle α, as well as the recent determinations of the CKM matrix elements $|V_{cb}|$ and $|V_{ub}|$ using semileptonic B decays.

Third Italian Workshop on the Physics at High Intensity (WIFAI2024)
12-15 November 2024
Bologna, Italy

*Speaker

© Copyright owned by the author(s) under the terms of the Creative Commons Attribution-NonCommercial-NoDerivatives 4.0 International License (CC BY-NC-ND 4.0) All rights for text and data mining, AI training, and similar technologies for commercial purposes, are reserved. ISSN 1824-8039 . Published by SISSA Medialab.

PoS(WIFAI2024)001

1. Introduction

Hadronic and semileptonic B decays provide precise constraints on the parameters of the Cabibbo-Kobayashi-Maskawa (CKM) quark-mixing matrix and are sensitive probes of physics beyond the Standard Model (SM).

Belle II [1] is a particle detector designed to study 7-on-4 GeV e^+e^- collisions around the $\Upsilon(4S)$ resonance. These collisions, produced with very high luminosity by the SuperKEKB collider at the KEK laboratory in Japan [2], predominantly result in $\Upsilon(4S) \to B\bar{B}$ decays, with low background contamination. Belle II began collecting physics data in March 2019 and provides competitive, unique, or world-leading sensitivity to key observables in hadronic and semileptonic B decays.

In this document, we present the measurement of $B^0 \to \rho^+\rho^-$ and $B^0 \to \pi^0\pi^0$ decays at Belle II that contributes to the determination of the CKM angle $\alpha = \arg\left(-\frac{V_{td}V_{tb}^*}{V_{ud}V_{ub}^*}\right)$, a limiting factor in the precision of SM tests based on global fits of the quark-mixing matrix unitarity. To suppress background, we employ binary classifiers C based on boosted decision trees (BDT) [3], which exploit differences in event topology. Continuum-background events tend to produce particles collimated into back-to-back jets, whereas $e^+e^- \to \Upsilon(4S) \to B\bar{B}$ events exhibit a more spherical shape. The determination of signal yields primarily relies on observables that take advantage of at-threshold production properties: the energy difference between the B candidate and the beam energy, ΔE, and the beam-constrained mass, M_{bc}, defined as

$$\Delta E = E_B^* - E_{\text{beam}}^*\,, \qquad M_{\text{bc}} = \sqrt{E_{\text{beam}}^{*2}/c^4 - (\boldsymbol{p}_B^*/c)^2}\,, \tag{1}$$

where E_B^* and $\boldsymbol{p}_B^*$ are the energy and momentum of the B candidate, and E_{beam}^* is the beam energy, all in the center-of-mass frame.

We also present measurements of semileptonic B-meson decays via the quark transitions $b \to c\ell\nu_\ell$ and $b \to u\ell\nu_\ell$ that provide instead an excellent sensitivity to the CKM matrix elements $|V_{cb}|$ and $|V_{ub}|$, respectively. The exclusive determinations of these quantities rely on the analysis of specific decay channels, such as $B \to D\ell\nu$, $B \to D^*\ell\nu$ and $B \to \rho\ell\nu$, $B \to \pi\ell\nu$ for the determinations of $|V_{cb}|$ and $|V_{ub}|$, respectively. Signal yields for extracting $|V_{cb}|$ element are usually determined by fitting key kinematic variables like: the angle between the B and $Y = D\ell$ directions, $\cos\theta_{BY}$, and the mass difference between the D^* and D mesons, ΔM, defined as

$$\cos\theta_{BY} = \frac{2E_B^*E_Y^* - m_B^2 - m_Y^2}{2|p_B^*||p_Y^*|}\,, \qquad \Delta M = M(D^*) - M(D). \tag{2}$$

Signal yields for extracting $|V_{ub}|$ element are determined using M_{bc} and ΔE observables. These variables are analyzed in bins of relevant kinematic observables, such as the recoil parameter, $w = E(D^*)/M(D^*)$ in the B rest frame or the squared four-momentum transfer q^2, as well as helicity angles. The CKM elements $|V_{cb}|$ and $|V_{ub}|$ are then extracted through a χ^2 fit to the differential decay rates measured in these bins, incorporating external inputs—typically from lattice QCD—to set the normalization and improve the precision of the extraction.

PoS(WIFAI2024)001

2. Toward CKM angle α

With an uncertainty of about 5%, the CKM angle α is currently among the major limiting factors on the global precision of the Unitarity Triangle. Belle II has the unique capability of measuring all $B \to \rho\rho$ and $B \to \pi\pi$ decays, from which α is determined. The combined information from these decays exploits isospin symmetry, reducing the effect of hadronic uncertainties. In these analyses, the B candidates are required to have $M_{\rm bc} > 5.27$ GeV/c^2 and $|\Delta E| < 0.15$ GeV (< 0.30 GeV for final states involving neutral pions), followed by continuum suppression that removes 90%-99% of this background component.

2.1 Measurement of the branching fraction and *CP*-violating asymmetry of the decay $B^0 \to \pi^0\pi^0$

We present a measurement of the branching fraction and time-integrated *CP* asymmetry (A_{CP}) for the $B^0 \to \pi^0\pi^0$ decay using a 365 fb^{-1} sample of electron-positron collision data.

The principal experimental challenge is the reconstruction of a rare decay in a final state with no charged particles, $B^0 \to \pi^0(\to \gamma\gamma)\pi^0(\to \gamma\gamma)$. The reconstruction of photons is based solely on calorimeter information.

To measure A_{CP}, the B-signal flavor (q) is assigned in each event by determining statistically the flavor of the accompanying neutral B meson (tagging). The branching fraction and A_{CP} are determined with a likelihood fit of the unbinned distributions of M_{bc}, ΔE, the output of the continuum-suppressing BDT, C_t, and the modified probability of wrongly assigned flavor, w_t. The signal distribution peaks in each fit observable as shown in Fig. 1.

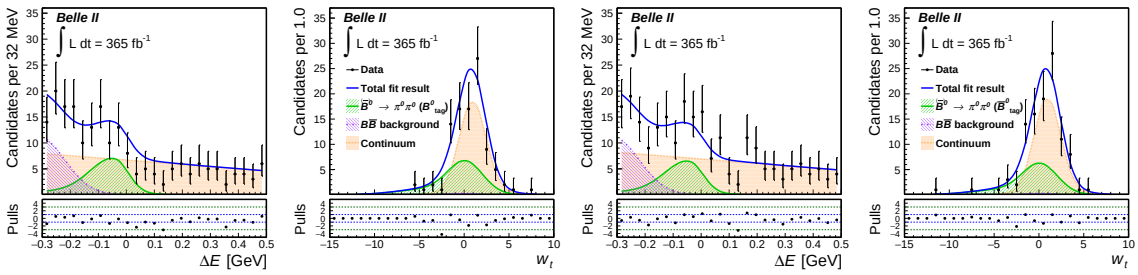

Figure 1: Signal-enhanced distributions of ΔE and w_t for $B^0 \to \pi^0\pi^0$ signal candidates with (left) positive and (right) negative q tags reconstructed in data, with fit projections overlaid. Lower panels show pulls.

The final results are [4]

$$\mathcal{B}(B^0 \to \pi^0\pi^0) = (1.25 \pm 0.20 \pm 0.11) \times 10^{-6}\,, \tag{3}$$

$$\mathcal{A}_{cp}(B^0 \to \pi^0\pi^0) = 0.03 \pm 0.30 \pm 0.04\,, \tag{4}$$

where the first contributions to the uncertainties are statistical and the second systematic. The (statistical) linear correlation between these two quantities is +1.5%. This work supersedes a previous Belle II result based on about one-half of the data sample [3], and incorporates a number of enhancements. These improvements reduce the fractional systematic uncertainty on the branching fraction by 40% and both the absolute statistical and systematic uncertainty on the A_{CP} by 3%, for a given sample size.

PoS(WIFAI2024)001

We reduce by 10° the 68% CL exclusion interval surrounding the CKM-favored solution, corresponding to a 30% fractional increase in ϕ_2 precision [5]. This makes the precision of ϕ_2 determinations based on $B \to \pi\pi$ decays competitive with the precision of $B \to \rho\rho$ determinations, resulting in a global improvement on the ϕ_2 precision.

2.2 Measurement of the branching fraction and *CP*-violating asymmetry of the decay $B^0 \to \rho^+\rho^-$

We present the measurement of $B^0 \to \rho^+\rho^-$ using a 365 fb^{-1} sample of electron-positron collision data. The measurement requires a complex angular analysis. Signal yields are determined with an unbinned maximum-likelihood fit of ΔE, the output of the continuum-suppressing BDT τ_C, two dipion masses and the two cosines of helicity angles of the ρ candidates. The helicity angle is the angle between the momentum difference of the ρ final states in the frame of the ρ, and the momentum of the ρ in the lab frame. The distributions of ΔE and cosine of the helicity angle of the $\rho^\pm$ candidates for $B^0 \to \rho^+\rho^-$ decays are shown in Fig. 2.

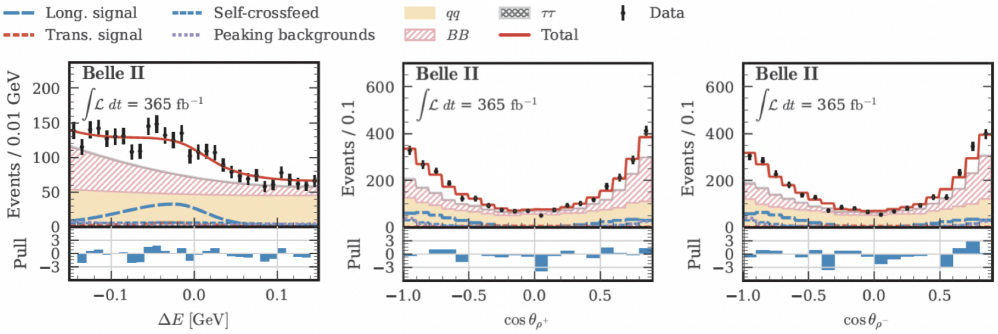

Figure 2: Distributions of ΔE (left) and $\cos\theta_{\rho^\pm}$ (center, right) for $B^0 \to \rho^+\rho^-$ decays. The points with error bars represent the data and the solid red curves show the sum of all contributions.

We measured the branching fraction and longitudinal polarization fraction for $B^0 \to \rho^+\rho^-$ decays as well as CP violation parameters for the longitudinal polarized decay [6]

$$\mathcal{B}(B^0 \to \rho^+\rho^-) = (2.88^{+0.23\,+0.29}_{-0.22\,-0.27}) \times 10^{-5}\,, \tag{5}$$

$$f_L = 0.921^{+0.024\,+0.017}_{-0.025\,-0.015}\,, \tag{6}$$

$$S = -0.26 \pm 0.19 \pm 0.08\,, \tag{7}$$

$$C = -0.02 \pm 0.12^{+0.06}_{-0.05}. \tag{8}$$

The results are in good agreement with the previous measurements from BaBar [7] and Belle [8].

3. Measurements of $|V_{cb}|$ and $|V_{ub}|$

Precise determinations of the CKM matrix elements $|V_{cb}|$ and $|V_{ub}|$ are essential for testing the SM and gaining deeper insight into the dynamics of weak decays. These elements can be extracted from semileptonic B-meson decays, which offer a theoretically clean framework to study the underlying quark transitions. In this context, Belle II has recently performed new measurements

PoS(WIFAI2024)001

of $B \to D\ell\nu$ and $B \to D^*\ell\nu$ for $|V_{cb}|$, as well as $B \to \rho\ell\nu$ and $B \to \pi\ell\nu$ for $|V_{ub}|$. These measurements contribute to reducing theoretical and experimental uncertainties, providing crucial inputs for precision tests of CKM unitarity and the study of hadronic effects in semileptonic transitions.

3.1 Measurement of $|V_{cb}|$ using $B \to D\ell\nu_\ell$ decay

We present the determination of the magnitude of the CKM matrix element $|V_{cb}|$ using $B \to D\ell\nu$ decays from 189 fb^{-1} sample of electron-positron collision data. The semileptonic decays $B^0 \to D^-(\to K^+\pi^-\pi^-)\ell^+\nu$ and $B^+ \to \overline{D^0}(\to K^+\pi^-)\ell^+\nu$ are reconstructed, where ℓ is either electron or a muon. The second B meson in the $\Upsilon(4S)$ event is not explicitly reconstructed. The signal yield in the reconstructed samples is extracted by performing a binned maximum likelihood fit to the $\cos\theta_{BY}$ distribution.

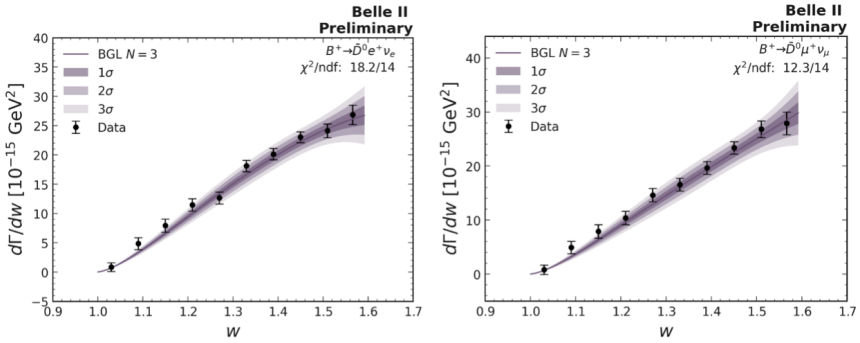

Figure 3: Observed $B^0 \to \overline{D}^0\ell^+\nu$ differential decay rates as functions of w with results of a combined fit to experimental and lattice QCD (FNAL/MILC and HPQCD) data. The fit results are shown separately for the electron and muon samples.

To determine the CKM parameter $|V_{cb}|$, we perform a combined χ^2 fit to the BGL form factor and lattice QCD calculation of form factors at w>1 by measuring the differential decay rates in 10 bins of w as show in Fig. 3. Assuming the electroweak correction $\eta_{EW} = 1.0066 \pm 0.0050$ [9], we finally obtain [10]

$$|V_{cb}| = (38.28 \pm 1.16) \times 10^{-3}, \tag{9}$$

in agreement with current world average estimates [12].

3.2 Measurement of $|V_{cb}|$ using $\overline{B}^0 \to D^{*+}\ell^-\overline{\nu_\ell}$ decay

We present the analysis of the semileptonic $\overline{B}^0 \to D^{*+}\ell^-\overline{\nu_\ell}$ decay, using a 189 fb^{-1} sample of electron-positron collision data, which is a usual benchmark channel to determine $|V_{cb}|$ due to the sizeable branching fraction, small backgrounds, and the availability of lattice QCD information at and beyond zero recoil.

We reconstruct the decays with the subsequent $D^{*+} \to D^0\pi^+$ and $D^0 \to K^-\pi^+$ decays, without explicit reconstruction of the other B meson produced in the $e^+e^- \to \Upsilon(4S) \to B^0\overline{B}^0$ process. The signal yield is extracted using two-dimensional likelihood fits to the binned $\cos\theta_{BY}$ and ΔM distributions, for the electron and muon final states. The measurement of partial decay rates in

PoS(WIFAI2024)001

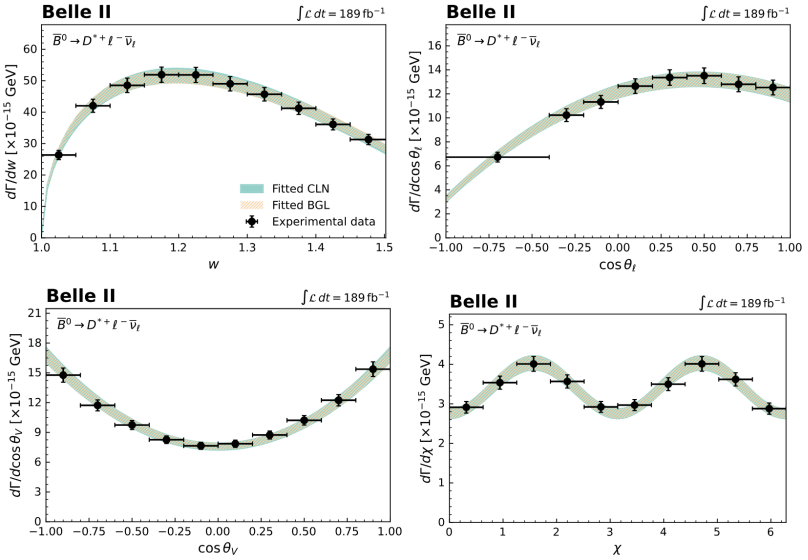

Figure 4: Comparison of the fitted partial decay rates with 1σ uncertainties in the BGL and CLN parametrizations to the unfolded experimental data (shown as points with error bars). Note that the BGL (hatched) band almost completely overlaps the CLN (solid) band.

bins of the recoil parameter w and the decay angles is carried out in two steps. First, backgrounds are determined using a likelihood fit and subtracted in each bin independently. The effects of the reconstruction resolution, efficiency, and detector acceptance are then corrected using the so-called "unfolding" procedure.

By summing the partial decay rates of all kinematic variables we obtain the total rate. The total decay rates averaged over w, $\cos\theta_\ell$, $\cos\theta_V$, and χ are converted to branching fractions using the B^0 lifetime. We average the electron and muon rates and analyze the observed decay rate. We perform the $|V_{cb}|$ measurement by performing a χ^2 of the partial decay rate as functions of the form-factor parameters and $|V_{cb}|$. We perform the fit assuming both the BGL and CLN form-factor parametrizations. Fig 4 compares the measured partial decay rates with the fitted differential decay rates. These spectra have very similar shapes for both parametrizations. Using the LQCD input at zero recoil, $\mathcal{F}(1) = 0.906 \pm 0.013$ [11] and the electroweak correction, $\eta_{EW} = 1.0066 \pm 0.0050$ [9] we determine [13]

$$|V_{cb}|_{\text{BGL}} = (40.57 \pm 0.31 \pm 0.95 \pm 0.58) \times 10^{-3}\,, \tag{10}$$

$$|V_{cb}|_{\text{CLN}} = (40.13 \pm 0.27 \pm 0.93 \pm 0.58) \times 10^{-3}\,, \tag{11}$$

where the first, second, and third contributions to the uncertainties are statistical, systematic, and from the prediction of $\mathcal{F}(1)$, respectively. The $|V_{cb}|$ results are in good agreement with the world average [12].

3.3 Measurement of $|V_{ub}|$ using $B^0 \to \pi^-\ell^+\nu_\ell$ and $B^+ \to \rho^0\ell^+\nu_\ell$ decays

We present a simultaneous measurement of $B^0 \to \pi^-\ell^+\nu_\ell$ and $B^+ \to \rho^0\ell^+\nu_\ell$ decays using a 365 fb^{-1} sample of electron-positron collision data that yields to a new determination of $|V_{ub}|$ while accounting for decays of one type that are reconstructed as the other. We simultaneously reconstruct

PoS(WIFAI2024)001

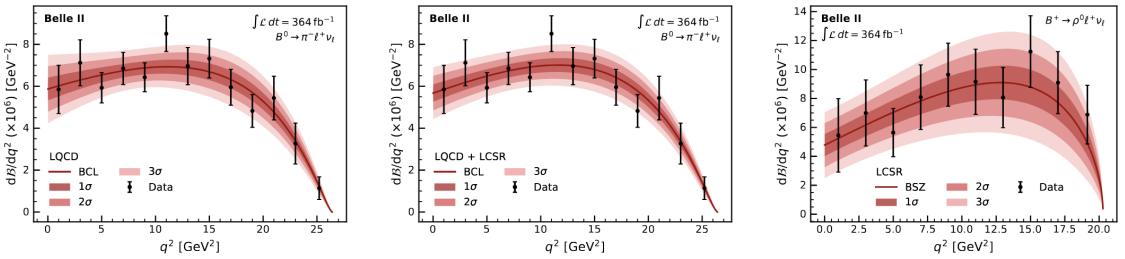

(a) (b) (c)

Figure 5: Measured partial branching fractions as a function of q^2 for $B^0 \to \pi^- \ell^+ \nu_\ell$ (a,b) and $B^+ \to \rho^0 \ell^+ \nu_\ell$ (c). The fitted differential rates are shown together with the one, two, and three standard-deviation uncertainty bands for fits using constraints on the form factors from (a) LQCD, (b) LQCD and LCSR, and (c) LCSR predictions.

$B^0 \to \pi^- \ell^+ \nu_\ell$ and $B^+ \to \rho^0 \ell^+ \nu_\ell$ focusing on decays with entirely charged final states in order to avoid backgrounds associated with neutral particles. For both modes we build three-dimensional histograms of the two kinematic variables M_{bc} and $|\Delta E|$ and the reconstructed q^2. From simulation, we define $B^0 \to \pi^- \ell^+ \nu_\ell$ and $B^+ \to \rho^0 \ell^+ \nu_\ell$ signal categories based on 13 and 10 disjoint bins of simulated q^2, respectively. We extract signal yields in all 23 signal categories with a simultaneous extended maximum-likelihood fit to both histograms. From these, we obtain differential branching fractions as functions of true q^2. We extract $|V_{ub}|$ separately from $B^0 \to \pi^- \ell^+ \nu_\ell$ and $B^+ \to \rho^0 \ell^+ \nu_\ell$ by performing χ^2 fits to the measured q^2 spectra, incorporating constraints from theoretical form-factor predictions based on unquenched lattice QCD and light-cone sum rule (LCSR) calculations.

The results are [14]

$$|V_{ub}|^{\mathrm{LQCD}}_{B\to\pi\ell\nu_\ell} = (3.93 \pm 0.09 \pm 0.13 \pm 0.19) \times 10^{-3}, \tag{12}$$

$$|V_{ub}|^{\mathrm{LQCD+LCSR}}_{B\to\pi\ell\nu_\ell} = (3.73 \pm 0.07 \pm 0.07 \pm 0.16) \times 10^{-3}, \tag{13}$$

$$|V_{ub}|^{\mathrm{LCSR}}_{B\to\rho\ell\nu_\ell} = (3.19 \pm 0.12 \pm 0.17 \pm 0.26) \times 10^{-3}, \tag{14}$$

where for all quoted $|V_{ub}|$ results the first uncertainty is statistical, the second is systematic and the third is theoretical. Fig. 5 shows the measured and fitted differential rates of $B^0 \to \pi^- \ell^+ \nu_\ell$ and $B^+ \to \rho^0 \ell^+ \nu_\ell$. The $|V_{ub}|$ results obtained from $B^0 \to \pi^- \ell^+ \nu_\ell$ are consistent with previous exclusive measurements [12]. The result obtained from $B^+ \to \rho^0 \ell^+ \nu_\ell$ is lower, but consistent with previous $|V_{ub}|$ determinations from $B \to \rho \ell \nu_\ell$ decays [15].

4. Summary

Recent Belle II measurements provide world-leading or highly competitive determinations of key CKM parameters. The new results on the CKM angle α from two-body B-meson decays represent some of the most precise measurements to date. Similarly, the latest determinations of $|V_{cb}|$ and $|V_{ub}|$ from semileptonic B decays are competitive with the most precise in the world, contributing significantly to the understanding of CKM unitarity. With increasing statistics and improved analysis techniques, Belle II continues to play a crucial role in testing the SM and searching for potential signs of new physics.

PoS(WIFAI2024)001

References

[1] T. Abe et al. (Belle Collaboration), *Belle II Technical Design Report* (2010), arXiv:1011.0352.

[2] Kazunori Akai et al., *SuperKEKB collider*, *Nucl. Instrum. Meth.* A **907**, 188 (2018).

[3] Abudinén, F. et al. (Belle II Collaboration), *Measurement of the branching fraction and CP asymmetry of* $B^0 \to \pi^0\pi^0$ *decays using* 198×10^6 $B\overline{B}$ *pairs in Belle II data* (2023), *Phys. Rev.* D **107**, 112009 (2023).

[4] I. Adachi et al. (Belle II Collaboration), *Measurement of the branching fraction and CP-violating asymmetry of the decay* $B^0 \to \pi^0\pi^0$ *using* 387 *million bottom-antibottom meson pairs in Belle II data* (2024), arXiv:2412.14260.

[5] Amhis, Y. et al. (Heavy Flavor Averaging Group Collaboration), *Averages of b-hadron, c-hadron, and* τ*-lepton properties as of 2021* (2023), *Phys. Rev.* D **107**, 052008 (2023).

[6] I. Adachi et al. (Belle II Collaboration), *Measurement of the branching fraction, polarization, and time-dependent CP asymmetry in* $B^0 \to \rho^+\rho^-$ *decays and constraint on the CKM angle* ϕ_2 (2024), arXiv:2412.19624.

[7] Aubert, B. et al. (BaBar Collaboration), *Study of* $B^0 \to \rho^+\rho^-$ *decays and constraints on the CKM angle* α (2007), *Phys. Rev.* D **76**, 052007 (2007).

[8] Vanhoefer, P. et al. (Belle Collaboration), *Study of* $B^0 \to \rho^+\rho^-$ *decays and implications for the CKM angle* ϕ_2 (2016), *Phys. Rev.* D **93**, 032010 (2016) [Erratum: *Phys. Rev.* D **94**, 099903 (2016).

[9] A. Sirlin, *Large* m_W, m_Z *behaviour of the* $O(\alpha)$ *corrections to semileptonic processes mediated by W* (1982), *Nucl. Phys.* B **196**, 83 (1982).

[10] Abudinén, F. et al. (Belle II Collaboration), *Determination of* $|V_{cb}|$ *from* $B \to D\ell\nu$ *decays using 2019-2021 Belle II data* (2022), arXiv:2210.13143.

[11] Bazarov, A. et al. (Fermilab Lattice and MILC Collaborations), *Semileptonic form factors for* $B \to D^*\ell\nu$ *at nonzero recoil from 2+1-flavor lattice QCD* (2022), *Eur. Phys. J.* C **82**, 1141 (2022).

[12] Sw. Banerjee et al. (The Heavy Flavor Averaging Group), *Averages of b-hadron, c-hadron, and* τ*-lepton properties as of 2023* (2024), arXiv:2411.18639.

[13] Adachi, I. et al. (Belle II Collaboration), *Determination of* $|V_{cb}|$ *using* $\overline{B}^0 \to D^{*+}\ell^-\overline{\nu}_\ell$ *decays with Belle II* (2023), *Phys. Rev.* D **108**, 092013 (2023).

[14] I. Adachi et al. (Belle II Collaboration), *Determination of* $|V_{ub}|$ *from simultaneous measurements of untagged* $B^0 \to \pi^-\ell^+\nu_\ell$ *and* $B^+ \to \rho^0\ell^+\nu_\ell$ *decays* (2024), arXiv:2407.17403.

[15] Bernlochner, Florian U. and Prim, Markus T. and Robinson, Dean J.,$B \to \rho l\overline{\nu}$ *and* $\omega l\overline{\nu}$ *in and beyond the Standard Model: Improved predictions and* $|V_{ub}|$ (2021), *Phys. Rev.* D **104**, 034032 (2021).

PoS(WIFAI2024)001